Clinical Oncology 31 (2019) 41–49

Contents lists available at ScienceDirect

Clinical Oncology

journal homepage: www.clinicaloncologyonline.net

Original Article

Evaluation of Response to Stereotactic Radiosurgery in Brain Metastases Using Multiparametric Magnetic Resonance Imaging and a Review of the Literature

V. Sawlani [*,†], N. Davies [*], M. Patel [*,†], R. Flintham [*], C. Fong [*], G. Heyes [*], G. Cruickshank [*,†], N. Steven [*,†], A. Peet [†,‡], A. Hartley [*], H. Benghiat [*], S. Meade [*], P. Sanghera [*,†]

[*] *Queen Elizabeth Hospital Birmingham, University Hospitals Birmingham NHS Foundation Trust, Birmingham, UK*
[†] *Institute of Cancer and Genomic Sciences, College of Medical and Dental Sciences, University of Birmingham, Birmingham, UK*
[‡] *Birmingham Children's Hospital, Birmingham Women's and Children's NHS Foundation Trust, Birmingham, UK*

Received 27 April 2018; received in revised form 3 August 2018; accepted 16 August 2018

Abstract

Aims: Following stereotactic radiosurgery (SRS), brain metastases initially increase in size in up to a third of cases, suggesting treatment failure. Current imaging using structural magnetic resonance imaging (MRI) cannot differentiate between tumour recurrence and SRS-induced changes, creating difficulties with patient management. Combining multiparametric MRI techniques, which assess tissue physiological and metabolic information, has shown promise in answering this clinical question.
Materials and methods: Multiparametric MRI techniques, including spectroscopy, diffusion and perfusion imaging, were used for the differentiation of radiation-related changes and tumour recurrence after SRS for intracranial metastases in six cases. All patients presented with enlargement of the treated lesion, an increase in perilesional brain oedema and aggravation or appearance of neurological signs and symptoms from 7 to 29 weeks after primary treatment.
Results: Multiparametric imaging helped to differentiate features of tumour progression ($n = 4$) from radiation-related changes ($n = 2$). A low apparent diffusion coefficient (ADC) $<1000 \times 10^{-6}$ mm^2/s, high relative cerebral blood volume (rCBV) ratio > 2.1, high choline:creatine (Cho:Cr) ratio > 1.8 suggested tumour recurrence. A high ADC $> 1000 \times 10^{-6}$ mm^2/s, low rCBV ratio < 2.1, Cho:Cr ratio < 1.8 suggested SRS-induced radiation changes. Multiparametric MRI diagnosis was confirmed by histology or radiological and clinical follow-up.
Conclusion: Multiparametric MRI was helpful in the early identification of radiation-related changes and tumour recurrence and may be useful for monitoring treatment changes in intracranial neoplasms after SRS treatment.

Key words: Brain metastases; multiparametric MRI diffusion perfusion spectroscopy; stereotactic radiosurgery

Introduction

Stereotactic radiosurgery (SRS) is now a widely accepted treatment modality for selected brain metastases with favourable prognosis [1,2]. Improvements in systemic control, concerns with whole brain radiotherapy-associated neurotoxicity [2,3] and increased sensitivity imaging are contributing to greater use of SRS for brain metastases. However, difficulty exists in terms of how best to assess the subsequent imaging changes of SRS-treated brain metastases. This includes the modality and frequency of assessment, method of measurement, magnitude of change that defines response or progression and differentiation between tumour-related and treatment-related changes [4].

In a series of 500 brain metastases treated with SRS, Patel *et al.* [5] reported that one-third of the lesions had a transient size increase after treatment, starting as early as 6 weeks, and could be observed up to 15 months post-SRS. It is estimated that between 30 and 75% of radiographically enlarging SRS-treated brain metastases are due to radiation-related

Author for correspondence: V. Sawlani, Imaging Department, Queen Elizabeth Hospital Birmingham, University Hospitals Birmingham NHS Foundation Trust, Mindelsohn Way, Edgbaston, Birmingham B15 2GW, UK. Tel: +44-121-371-4754.
E-mail address: Vijay.Sawlani@uhb.nhs.uk (V. Sawlani).

https://doi.org/10.1016/j.clon.2018.09.003
0936-6555/

changes alone [6–11]. Given that early volume expansion may be relatively common, the value of short interval imaging and a 3 month response assessment, as carried out in many early phase studies, is called into question.

Current imaging using structural magnetic resonance imaging (MRI), which relies on contrast enhancement pattern changes and alterations in T2/fluid-attenuated inversion recovery (FLAIR) weighting, is insufficient and cannot differentiate local tumour recurrence from SRS-induced changes [4]. As such, more advanced MRI methods that can monitor physiological and metabolic properties of tumour are being used and investigated to address this question. These include diffusion-weighted imaging (DWI), perfusion-weighted imaging (PWI) and magnetic resonance spectroscopy (MRS). The parameters of interest considered here are apparent diffusion coefficient (ADC), relative cerebral blood volume (rCBV) and the relative metabolite levels, particularly the choline to creatine ratio (Cho:Cr) from MRS.

There are data supporting the utility of each of these methods [6,7,9,11], although limitations remain such that no method is currently validated as yielding the definitive MRI parameter of choice to distinguish between metastatic tumour recurrence and radiation-related changes. Combining these three methods in a multiparametric MRI protocol may provide a higher degree of confidence in gauging brain metastases response post-SRS. Through presentation of a small case series we discuss how advanced MRI techniques may be able to aid with response assessment after SRS for brain metastases, with a review of the literature.

Materials and Methods

A retrospective review was carried out of six patients with brain metastases enlarging at a relatively early time point after SRS, assessed with multiparametric MRI (Table 1). The use of multiparametric MRI was restricted to cases with early post-SRS enlargement and uncertainty at the multidisciplinary team meeting regarding progression versus post-SRS change. The inclusion criteria comprised of the criteria for commissioning for SRS in the UK: selection of patients by the multidisciplinary team with an understanding of systemic and neurological disease processes, pre-treatment tumour volume less than 20 cm^3, Karnofsky performance status ≥ 70 and a life expectancy expected to be greater than 6 months.

All SRS treatments were delivered using the CyberKnife® (Accuray®, Sunnyvale, California, USA) robotic SRS platform utilising circular field size apertures. Pre- and post-contrast high resolution (1 mm) computed tomography scans were carried out with the patient immobilised in a thermoplastic beam directional head shell. Each case was contoured by a clinical oncologist and peer approved by a neuroradiologist. The gross tumour volume was used to define the planning target volume without additional margin. The protocol for the prescription dose was 15–24 Gy in a single fraction guided by the planning target volume. The treatment was optimised such that the surface (prescribed dose) was at 60% of the maximum dose and a minimum 98% coverage with intended dose was required. The schedule for follow-up MRI scans was at 3-monthly intervals while clinically appropriate unless required earlier due to clinical reasons. Upon radiographic evidence of enlargement of at least one treated lesion by at least 20%, patients underwent MRI with diffusion, perfusion and spectroscopy techniques to aid differentiation between tumour progression versus radiation changes. Multiparametric MRI examinations were carried out to assess the enlarging lesion 7–29 weeks after SRS in these six patients. Primary tumour histology comprised of melanoma ($n = 3$), breast ($n = 2$) and non-small cell lung ($n = 1$). Patient 6 had a history of recent immune checkpoint inhibition (ICI) treatment (Ipilimumab), which ended 2 months before SRS, and further ICI (Pembrolizumab) after SRS, as described in Table 1; none of the other patients had a history of ICI. Multiparametric MRI features were then correlated with either histopathological or subsequent clinicoradiological findings.

Magnetic Resonance Imaging Protocol

MRI was carried out on a 3 T scanner (Magnetom Verio; Siemens, Erlangen, Germany) with a 32-channel phased-array head coil. Axial T2-weighted images, T2-weighted FLAIR and DWI of the whole brain were obtained. This was followed by dynamic susceptibility contrast-enhanced (DSC) perfusion imaging using gradient-echo echo-planar

Table 1
Patient and stereotactic radiosurgery (SRS) treatment information

Patient	Primary tumour histology	Number of lesions treated	SRS dose (Gy)	SRS volume (mm^3)	Interval from SRS to multiparametric MRI (weeks)	Concurrent or history of immunotherapy treatment
1	Breast	1	21	2329	24	None
2	Breast	2	21	1989	29	None
3	Non-small cell lung	2	21	1521	7	None
4	Melanoma	5	21	417	10	None
5	Melanoma	1	18	4745	13	None
6	Melanoma	1	18	5846	22	Pembrolizumab started 1 month after SRS. 3 month course of Ipilimumab (ended 2 months before SRS).

MRI, magnetic resonance imaging.

imaging (GE-EPI) during the first pass of a standard dose (7.5 mmol) bolus of gadolinium contrast (Gadovist, Bayer, Berlin, Germany) administered intravenously at a flow rate of 6 ml/s. In total, 80 volumes were acquired at 2.1 s intervals with the bolus typically arriving between the 10th and 15th volume. This was followed by post-contrast three-dimensional T1-weighted images (MPRAGE) acquired in the axial plane with sagittal and coronal reformats. Two-dimensional MRS imaging was then carried out in the axial plane, choosing a slice with the largest contrast-enhancing lesion area. Short echo (TE = 30 ms) and intermediate echo (TE = 135 ms) single-voxel MRS was also carried out in all cases.

Magnetic Resonance Imaging Post-processing and Analysis

ADC maps were calculated from the DWI on the magnetic resonance scanner software (Magnetom VB17; Siemens). DSC data were post-processed on a Siemens Leonardo workstation (software version VB17; Siemens) using a global AIF without T1 correction, producing maps of rCBV and relative cerebral blood flow. MRS data were processed and fitted using the magnetic resonance scanner software (Magnetom VB17; Siemens) to produce peak integral values for N-acetylaspartate (NAA), Cr, Cho and lipids. ADC and rCBV values for each treated metastasis were measured by a consultant neuroradiologist using regions-of-interest (ROIs) placed in a region of suspected disease progression (high rCBV). If no region of higher rCBV was observed, the ROI was instead placed in the largest area of contrast-enhancing tissue. rCBV values were normalised using a further ROI placed in equivalent tissue on the contralateral (normal) side. MRS data were used to determine the maximum observed ratio of Cho:Cr in any available voxel within the contrast-enhancing lesion.

Results

Quantitative Analysis

For quantitative analysis, the threshold values used to distinguish tumour recurrence from radiation-related changes for the multiparametric MRI parameters from DWI, PWI and MRS, respectively, were as follows: ADC $\leq 1000 \times 10^{-6}$ mm^2/s, rCBV ratio ≥ 2.1 and Cho:Cr ratio ≥ 1.8. Correlations between multiparametric MRI and longitudinal clinicoradiological outcome were investigated and are presented in Table 2 for all six patients.

With respect to longitudinal follow-up outcome, four of the six patients had progressive disease from the SRS-treated lesions. These were confirmed histopathologically ($n = 2$) or radiologically ($n = 2$). The other two patients had subsequent regression or stable disease on clinical and radiological follow-up.

When an rCBV threshold ratio of 2.1 was applied [7], we were able to divide our patients into either suspected tumour recurrence (rCBV > 2.1, $n = 3$) or suspected radiation-related changes (rCBV ≤ 2.1, $n = 3$). However, for the one patient in the 'suspected radiation-related changes group' with borderline rCBV of 1.9, the features of a high Cho:Cr ratio (2.6) and intermediate ADC (999×10^{-6} mm^2/s) were taken into account. These three parameters when considered together would predict a high likelihood of tumour recurrence, as opposed to radiation changes. Therefore, with the help of multiparametric MRI, four patients were deemed to have features of tumour progression, with the other two patients considered to have features of radiation-related changes. These multiparametric MRI findings were concordant with the subsequent longitudinal clinicoradiological outcomes.

Descriptive Analysis

Four cases (Figures 1–4) are presented showing multiparametric MRI findings in true progression and radiation-related changes.

Discussion

The small number of cases presented here have been used to illustrate how multiparametric MRI may be useful in the evaluation of post-SRS change for brain metastases. The use of these combined techniques has strongly influenced

Table 2
Post-stereotactic radiosurgery multiparametric magnetic resonance imaging (MRI) results with clinicoradiological follow-up

Patient	DWI	PWI	MRS (TE 30 ms)	Imaging follow-up (time and outcome)
	ADC ($\times 10^{-6}$ mm^2/s)	rCBV ratio (lesion/contralateral)	Maximum Cho:Cr	
1	920	5.1	2.8	6 months – disease progression
2	999	1.9	2.6	6 months – progression confirmed with resection
3	1479	0.9	1.0	6 months – stable
4	628	4.5	2.0	Progression on computed tomography and clinical deterioration
5	1159	2.1	1.6	4 months – regression of disease
6	564	3.1	5.7	3 months – progression confirmed with resection

DWI, diffusion-weighted imaging; ADC, apparent diffusion coefficient; PWI, perfusion-weighted imaging; rCBV, relative cerebral blood volume; MRS, magnetic resonance spectroscopy; Cho:Cr, choline to creatine ratio.

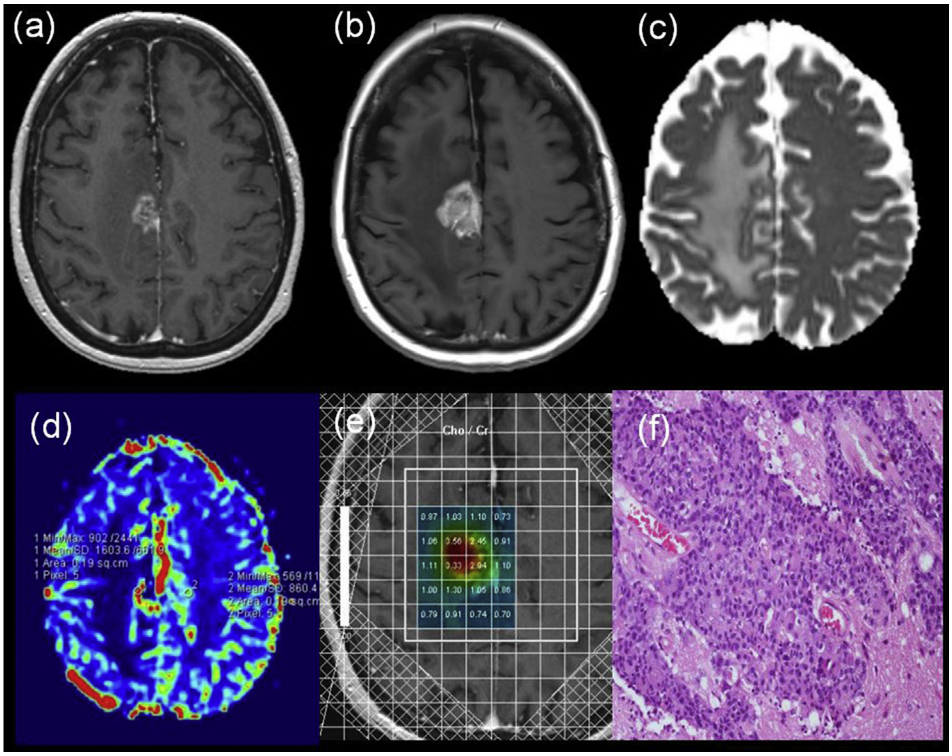

Fig 1. Patient 2: brain metastasis from primary breast carcinoma. (a) Brain metastasis in the right mesial frontal lobe shown on axial T1-weighted post-contrast magnetic resonance imaging (MRI). (b) Post-stereotactic radiosurgery scan at 29 weeks showed more than 20% increase in the lesion size with associated oedema. Multiparametric MRI showed: (c) a low apparent diffusion coefficient (ADC; 999×10^{-6} mm^2/s) on diffusion-weighted imaging (DWI), (d) a borderline relative cerebral blood volume (rCBV) ratio (1.9) on perfusion-weighted imaging and (e) a high choline to creatine ratio (Cho:Cr; 2.6) on magnetic resonance spectroscopy (MRS; TE = 35 ms). Two of the three parameters (DWI and MRS) suggested poor response and disease progression. (f) Surgical decision was taken to operate on the motor cortex. Excision of the right frontal tumour was carried out. Microscopy showed increased mitoses and tumour cells with large nuclei and area of necrosis. Oestrogen receptor was also positive, consistent with the known breast carcinoma primary.

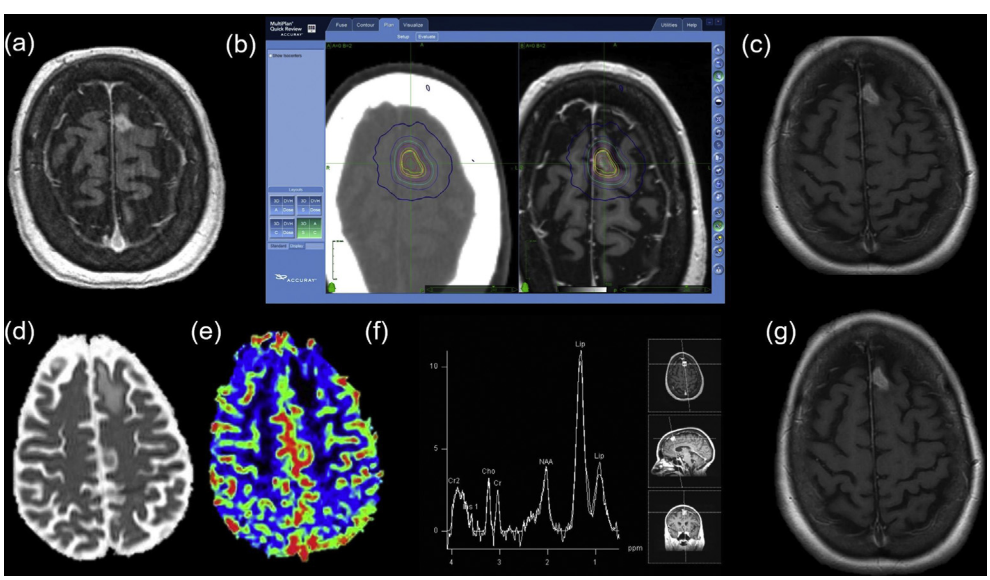

Fig 2. Patient 3: brain metastasis from primary non-small cell lung carcinoma. (a) Brain metastasis in left frontal lobe shown on axial T1-weighted post-contrast magnetic resonance imaging (MRI). (b) Dose distribution on stereotactic radiosurgery (SRS) planning scan. (c) Post-SRS scan at 7 weeks showed more than 20% increase in lesion size. Multiparametric MRI showed: (d) a high apparent diffusion coefficient (ADC; 1479×10^{-6} mm^2/s) on diffusion-weighted imaging, (e) a low relative cerebral blood volume (rCBV) ratio (0.9) on perfusion-weighted imaging and (f) a low choline to creatine ratio (Cho:Cr; 1.0) and very high lipid on magnetic resonance spectroscopy. All parameters suggested good response to SRS. (g) Post-SRS post-contrast T1-weighted scan at 24 weeks showed no further increase in lesion size and the patient remained clinically stable.

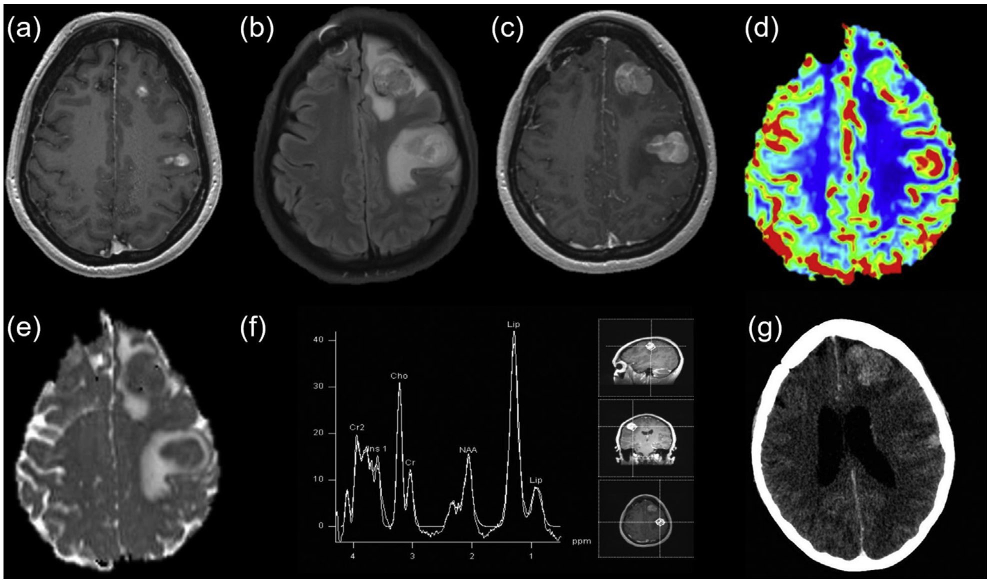

Fig 3. Patient 4: melanoma with brain metastases. (a) Three small enhancing lesions in left frontal lobe visible on axial T1 post-contrast magnetic resonance imaging (MRI). (b,c) Post-stereotactic radiosurgery T2-fluid-attenuated inversion recovery and post-contrast T1-weighted scans showed an increase in size and oedema in all the lesions. Multiparametric MRI showed: (d) a high relative cerebral blood volume (rCBV) ratio (4.5) on perfusion-weighted imaging, (e) a low apparent diffusion coefficient (ADC; 629 $\times$ 10^{-6} mm^2/s) on diffusion-weighted imaging and (f) a very high choline to creatine ratio (Cho:Cr; 2.6) and a moderate amount of lipid on magnetic resonance spectroscopy. All parameters suggested a poor response to treatment and disease progression. (g) Follow-up post-contrast computed tomography head study showed a further increase in the size of the lesions, suggesting disease progression.

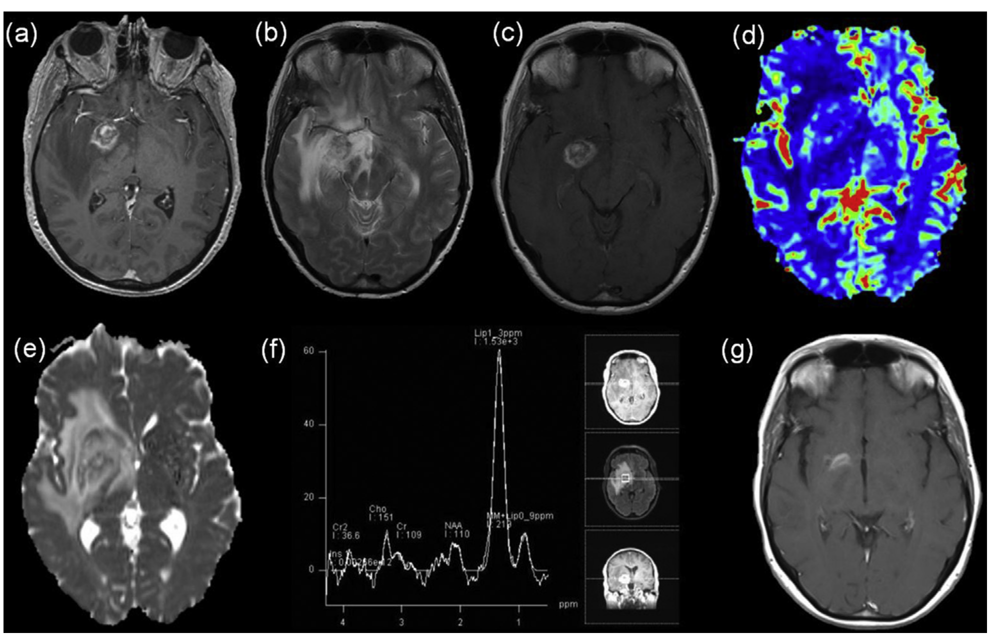

Fig 4. Patient 5: melanoma metastasis. (a) One enhancing lesion in the right basal ganglion visible on axial T1 post-contrast magnetic resonance imaging (MRI). (b,c) Post-stereotactic radiosurgery T2-weighted and post-contrast T1-weighted scans showed greater than 20% increase in lesion size and associated oedema. Multiparametric MRI showed: (d) a low relative cerebral blood volume (rCBV) ratio (2.1) on perfusion-weighted imaging, (e) a high apparent diffusion coefficient (ADC; 1159 $\times$ 10^{-6} mm^2/s) and (f) a low choline to creatine ratio (Cho:Cr; 1.6) and very high lipid. Most parameters suggested a good response. (g) Follow-up post-contrast T1-weighted scan showed regression of the lesion.

clinical decision-making and treatment options for patients. In the case of multiparametric MRI suggesting tumour progression, the decision to operate has been made, despite the lesion being located in the motor cortex, with histology confirming tumour progression (Patient 2, Figure 1). In addition, for a patient who was unsuitable for further treatment with suggestion of disease progression on multiparametric MRI, the decision for palliative treatment to be started was made, without further follow-up MRI (Patient 4, Figure 3). Where multiparametric MRI was suggestive of a good response to SRS, confidence was given for clinical decisions to be made to follow up patients through routine imaging (Patient 3, Figure 2), particularly in the case where the lesion was located in an eloquent area and close to the basal ganglia, which would make surgical intervention risky (Patient 5, Figure 4).

The mechanism of treatment effect after SRS is not yet well understood, although it is thought that microvascular damage is induced, which leads to indirect tumour cell death [12]. The subsequent release of cell death toxins is thought to lead to a spread of vasogenic fluid into the brain parenchyma with associated inflammation, oedema and abnormal vessel permeability [13]. As with glioblastoma, serial structural MRI is the standard method of assessing response after radiosurgery to brain metastases. However, at single time points of imaging using current structural MRI techniques, it can be virtually impossible to differentiate tumour progression from radiation changes or a mixture of both [10].

In recognition of the increasing proportion of patients with brain metastases treated with more aggressive local treatment, and the increasing inclusion of this patient cohort in clinical trials, the international multidisciplinary Response Assessment in Neuro-Oncology Brain Metastases (RANO-BM) working group has recently published a guideline on standard response and progression criteria based on MRI [4]. The addition of ICI alongside SRS for brain metastases further complicates imaging follow-up assessment. Some studies have identified prolonged survival in the subgroup of patients whose SRS-treated brain metastases show initial enlargement [14,15], possibly due to a synergy between ICI and radiotherapy [16]. As such, the stakes on timely and accurate interpretation of post-SRS follow-up imaging are high. Presumed progression might lead to unnecessary additional treatment to the local site, or discontinuation of the earlier efficacious systemic therapies, or confound the outcomes of clinical trials examining new systemic treatment for patients with treated brain metastases. In this cohort, the patient with a history of ICI showed features of progression on multiparametric MRI and follow-up. In view of the clinical significance and implications of accurately differentiating radiation changes from genuine tumour progression, various MRI parameters are being investigated, of which PWI, DWI and MRS are the most promising.

Tumour recurrence is associated with increased angiogenesis and its resultant region of hyperperfusion with higher blood volume. Radiation-related changes, often confusingly and synonymously used with ‘radiation necrosis’ in the literature, on the other hand, are associated with regions of hypoperfusion due to radiation-induced vascular endothelial damage and coagulative necrosis [14,17]. rCBV, which is the calculated CBV relative to the contralateral (normal) brain, is the most widely used parameter derived from DSC and is considered a marker of angiogenesis. rCBV has been consistently reported to be a promising magnetic resonance perfusion parameter for differentiating tumour recurrence (higher rCBV values due to increased angiogenic hyperperfusion) against radiation changes (lower rCBV values) in the context of radiosurgery-treated brain metastases [6–8,11]. Hoefnagals *et al.* [6] showed an optimum rCBV cut-off ratio of > 2.0 for tumour recurrence, with a sensitivity of 85% and a specificity of 71% and Mitsuya *et al.* [7] showed an optimum cut-off ratio of > 2.1, with an increased sensitivity of 100% and a specificity of 95.2%. Barajas *et al.* [11] also showed that all six subjects with rCBV < 1.35 had radiation changes only. In our case cohort, we applied the threshold rCBV of 2.1.

DWI is based on the ability of MRI to detect Brownian motion of water molecules within the microenvironment. In cases of tumour recurrence, there is a high concentration of malignant cells at the recurrence site, with increased cellularity and increased intracellular space. This situation restricts free water movement due to closely packed cell walls. Most studies on DWI and ADC are on intrinsic brain tumours. Cha *et al.* [18] retrospectively investigated the role of combined ADC and rCBV in differentiating radiation-induced changes and tumour progression in 16 patients with resected enlarging brain metastases following radiosurgery. They demonstrated a sensitivity of 100% and a specificity of 56% for differentiating radiation necrosis from tumour progression using these two techniques in combination [18]. Song *et al.* [19] defined an optimal ADC threshold value of 900×10^{-6} mm^2/s for differentiating between true progression and pseudoprogression in glioblastoma; in our cohort, based on our experience we applied a similar ADC threshold value of 1000×10^{-6} mm^2/s.

MRS measures the composition of various metabolites within a tissue [20]. These metabolites can be quantitatively evaluated singularly, or as a ratio, typically Cho:Cr and Cho:NAA in the context of brain tumours and metastases. In our case series, we used Cho:Cr with a threshold of > 1.8 for tumour recurrence, based on the findings from Weybright *et al.* [21] showing positive prediction in 27 of 28 cases in their study. Chernov *et al.* [9] conducted a study on 33 cases of SRS-treated brain metastases followed up with multivoxel MRS. Using MRS parameters of a NAA:Cho ratio $<$ 1.0 and a lipid:Cho ratio < 3.0 as cut-off values for tumour recurrence, they correctly identified patients into pure recurrence, partial recurrence, pure radionecrosis and peritumoural necrosis groups [9]. Six of the cases with subsequent resection information showed pathologico-MRS concordance. Huang *et al.* [8] found that the choline to contralateral normal choline ratio had the best performance and a cut-off value > 1.2 yielded 33% sensitivity and 100% specificity. A meta-analysis from six MRS studies concluded that using Cho:Cr or Cho:NAA ratios may increase the accuracy of differentiating radionecrosis from tumour recurrence, with stronger pooled effects for Cho:Cr [22].

Other MRI techniques have also been used to help with response assessment. A study by Zach *et al.* [23] using delayed contrast extravasation MRI more than 1 h after contrast injection has also showed potential for differentiating between tumour recurrence and radiation changes, with a sensitivity/PPV of 100%/89% in brain metastases.

However, no specificity or NPV was quoted [23]. The technique may also be particularly useful in haemorrhagic lesions when other techniques may be technically difficult to perform and interpret due to susceptibility artefact.

Multiparametric MRI adds relevant and important physiological and metabolic information about the tissue microenvironment alongside structural MRI findings in the quest to differentiate brain metastasis recurrence versus radiation changes. However, most studies thus far have investigated individual parameters independently, had limited subject numbers and are of a retrospective nature. A review of the literature has been carried out and the results are summarised in Table 3. The multiparametric MRI approach is being utilised in the context of primary brain tumours [22,29–32], although there is very sparse literature on multiparametric magnetic resonance assessment of post-SRS brain metastasis [33].

Prat *et al.* [34] suggested that magnetic resonance perfusion and MRS were the most promising imaging methods for detecting tumour recurrence and this is also reflected in the meta-analysis by Chuang *et al.* [22] indicating rCBV and Cho:Cr or Cho:NAA as good discriminators. In this small case series, rCBV was utilised to make a preliminary dichotomy of tumour recurrence versus radiation changes, then took Cho:Cr and ADC into account to more accurately interpret a case with borderline rCBV values. Table 4 summarises features of multiparametric MRI in relation to the probable tumour state.

Multiparametric MRI including rCBV for angiogenesis, ADC for movement of water molecules and Cho for membrane turnover provide assessment of the physiological and metabolic environment of the tissue. The RANO-BM working group has also encouraged the use of advanced imaging for assessing treatment response in the recently published

Table 3
Review of results from previous studies for differentiating tumour recurrence from radiation-related changes/necrosis in patients with brain metastases following radiosurgery

Reference	Test, parameter	Cut-off values	Tumour recurrence (TR)		Radiation change/ necrosis (RC)		Mixed – recurrence and necrosis	
			Sensitivity (%)	Specificity (%)	Sensitivity (%)	Specificity (%)	Sensitivity (%)	Specificity (%)
[24]	Conventional MRI, T1/T2 mismatch				83.3	91.1		
[25]	Conventional MRI, lesion quotient	<0.3 (RC), 0.3–0.6 (mixed), >0.6 (TR)	100	32	80	96	15	100
[26]	Conventional MRI, lesion quotient	<0.3 (RC), 0.3–0.6 (mixed), >0.6 (TR)	59	41	8	91	0	64
[7]	Perfusion MRI, rCBV	>2.1 (TR)	100	95.2				
[11]	Perfusion MRI, rCBV	<1.54 (RC)			91.3	72.73		
	Perfusion MRI, rPH	<0.69 (RC)			86.96	45.45		
	Perfusion MRI, PSR	>76.3 (RC)			95.65	100		
[27]	Conventional MRI, volume				64	43		
	Perfusion MRI, regional CBV				91	71		
[8]	Perfusion MRI, rCBV	>2 (TR)	56	100				
	MRS, rCho	1.2	33	100				
	Conventional MRI, volume	65%	100	80				
[28]	MRS, Cho/Lip	>0.3 (TR), <0.3 (RC)	PPV 94.4		PPV 100			
	MRS, Cho/Cr	>2.48 (TR), <2.48 (RC)	PPV 88.9		PPV 71.4			

MRI, magnetic resonance imaging; rCBV, relative cerebral blood volume; rPH, relative peak height; PSR, percentage signal recovery; MRS, magnetic resonance spectroscopy; rCho, relative choline; Lip, lipid; Cr, creatine; PPV, positive predictive value.

Table 4
Multiparametric magnetic resonance imaging features for differentiating tumour recurrence from radiation-related changes

Imaging sequence	Tumour recurrence	Radiation-related change/necrosis
Diffusion-weighted imaging	Lower ADC values ($<1000 \times 10^{-6}$ mm^2/s)	Higher ADC values ($>1000 \times 10^{-6}$ mm^2/s)
Perfusion-weighted imaging	Elevated rCBV ratio (>2.1)	Decreased rCBV ratio (<2.1)
Magnetic resonance spectroscopy	Higher Cho:Cr (>1.8)	Lower Cho:Cr (<1.8)

ADC, apparent diffusion coefficient; rCBV, relative cerebral blood volume; Cho:Cr, choline to creatine ratio.

guideline [2]. However, they deemed that there was insufficient evidence for any one modality to be recommended in the recently published guideline [4], but from our limited experience we recommend the multiparametric approach. The adoption and widespread clinical use of multiparametric techniques is limited due to a number of factors. The technical issues include a lack of standardisation of acquisition techniques and availability of expertise. Further studies and funding are required to investigate the early post-SRS treatment response through a prospective trial with the inclusion of multiparametric MRI at baseline and 6–9 weeks after SRS treatment, although a single post-SRS multiparametric examination could also provide the necessary information for making clinical decisions. To allow for validation, the study should be carried out across multiple centres [13].

Conclusion

Response assessment after SRS for brain metastases remains challenging and no single supplementary MRI parameter can be recommended to help discriminate progression from SRS-related changes. Preliminary results from this study suggest that advanced imaging techniques, such as multiparametric MRI utilising rCBV from PWI, Cho:Cr from MRS and ADC from DWI, are feasible and hold promise for SRS-treated brain metastases in distinguishing tumour recurrence from radiation changes, with improved accuracy compared with any technique in isolation. However, prospective and longitudinal studies are required to validate multiparametric MRI prior to application in standard clinical practice.

Conflict of Interest

The authors declare no conflict of interest.

Acknowledgments

We are grateful to Mike Hammond, Chief Executive of the QEHB Charity for raising funds for the CyberKnife® robotic radiotherapy system which has been providing treatment to patients with brain metastases at UHB since 2013. We also acknowledge the radiographers Jane Herbert, Matthew Hartley and Steve Peplow for their help with this work.

Appendix A. Supplementary data

Supplementary data to this article can be found online at https://doi.org/10.1016/j.clon.2018.09.003.

References

[1] Andrews DW, Scott CB, Sperduto PW, Flanders AE, Gaspar LE, Schell MC, *et al*. Whole brain radiation therapy with or without stereotactic radiosurgery boost for patients with one to three brain metastases: phase III results of the RTOG 9508 randomised trial. *Lancet* 2004;363(9422):1665–1672.

[2] Brown PD, Ahluwalia MS, Khan OH, Asher AL, Wefel JS, Gondi V. Whole-brain radiotherapy for brain metastases: evolution or revolution? *J Clin Oncol* 2018;36(5):483–491.

[3] Sahgal A, Ruschin M, Ma L, Verbakel W, Larson D, Brown PD. Stereotactic radiosurgery alone for multiple brain metastases? A review of clinical and technical issues. *Neuro-oncology* 2017; 19(Suppl. 2):ii2–ii15.

[4] Lin NU, Lee EQ, Aoyama H, Barani IJ, Barboriak DP, Baumert BG, *et al*. Response assessment criteria for brain metastases: proposal from the RANO group. *Lancet Oncol* 2015;16(6):e270–e278.

[5] Patel TR, Mchugh BJ, Bi WL, Minja FJ, Knisely JP, Chiang VL. A comprehensive review of MR imaging changes following radiosurgery to 500 brain metastases. *AJNR Am J Neuroradiol* 2011;32(10):1885–1892.

[6] Hoefnagels FW, Lagerwaard FJ, Sanchez E, Haasbeek CJ, Knol DL, Slotman BJ, *et al*. Radiological progression of cerebral metastases after radiosurgery: assessment of perfusion MRI for differentiating between necrosis and recurrence. *J Neurol* 2009;256(6):87887.

[7] Mitsuya K, Nakasu Y, Horiguchi S, Harada H, Nishimura T, Bando E, *et al*. Perfusion weighted magnetic resonance imaging to distinguish the recurrence of metastatic brain tumors from radiation necrosis after stereotactic radiosurgery. *J Neurooncol* 2010;99(1):81–88.

[8] Huang BY, Kwock L, Castillo M, Smith JK. Association of choline levels and tumor perfusion in brain metastases assessed with proton MR spectroscopy and dynamic susceptibility contrast enhanced perfusion weighted MRI. *Technol Cancer Res Treat* 2010;9(4):32737.

[9] Chernov MF, Hayashi M, Izawa M, Usukura M, Yoshida S, Ono Y, *et al*. Multivoxel proton MRS for differentiation of radiation induced necrosis and tumor recurrence after gamma knife radiosurgery for brain metastases. *Brain Tumor Pathol* 2006;23(1):1927.

[10] Stockham AL, Suh JH, Chao ST, Barnett GH. Management of recurrent brain metastasis after radiosurgery. *Prog Neurol Surg* 2012;25:273–286.

[11] Barajas RF, Chang JS, Sneed PK, Segal MR, McDermott MW, Cha S. Distinguishing recurrent intra-axial metastatic tumor from radiation necrosis following Gamma Knife radiosurgery using dynamic susceptibility-weighted contrast-enhanced perfusion MR imaging. *AJNR Am J Neuroradiol* 2009;30:367–372.

[12] Park HJ, Griffin RJ, Hui S, Levitt SH, Song CW. Radiation-induced vascular damage in tumors: implications of vascular damage in ablative hypofractionated radiotherapy (SBRT and SRS). *Radiat Res* 2012;177(3):311–327.

[13] Walker AJ, Ruzevick J, Malayeri AA, Rigamonti D, Lim M, Redmond KJ, *et al*. Postradiation imaging changes in the CNS: how can we differentiate between treatment effect and disease progression? *Future Oncol* 2014;10(7):1277–1297.

[14] Kiess AP, Wolchok JD, Barker CA, Postow MA, Tabar V, Huse JT, *et al*. Stereotactic radiosurgery for melanoma brain metastases in patients receiving ipilimumab: safety profile and efficacy of combined treatment. *Int J Radiat Oncol Biol Phys* 2015; 92(2):368–375.

[15] Anderson ES, Postow MA, Wolchok JD, Young RJ, Ballangrud A, Chan TA, *et al*. Melanoma brain metastases treated with stereotactic radiosurgery and concurrent pembrolizumab display marked regression; efficacy and safety of combined treatment. *J Immunother Cancer* 2017;5(1):76.

[16] Chen L, Douglass J, Kleinberg L, Ye X, Marciscanco AE, Forde PM, *et al*. Concurrent immune checkpoint inhibitors

and stereotactic radiosurgery for brain metastases in non-small cell lung cancer, melanoma, and renal cell carcinoma. *Int J Radiat Oncol Biol Phys* 2018;100(4):916–925.

[17] Verma N, Cowperthwaite MC, Burnett MG, Markey MK. Differentiating tumor recurrence from treatment necrosis: a review of neuro-oncologic imaging strategies. *Neuro-oncology* 2013;15(5):515–534.

[18] Cha J, Kim ST, Kim HJ, Kim BJ, Jeon P, Kim KH, *et al*. Analysis of the layering pattern of the apparent diffusion coefficient (ADC) for differentiation of radiation necrosis from tumour progression. *Eur Radiol* 2013;23(3):879–886.

[19] Song YS, Choi SH, Park CK, Yi KS, Lee WJ, Yun TJ, *et al*. True progression versus pseudoprogression in the treatment of glioblastomas: a comparison study of normalized cerebral blood volume and apparent diffusion coefficient by histogram analysis. *Korean J Radiol* 2013;14(4):662–672.

[20] Horská A, Barker PB. Imaging of brain tumors: MR spectroscopy and metabolic imaging. *Neuroimaging Clin North Am* 2010;20(3):293–310.

[21] Weybright P, Sundgren PC, Maly P, Hassan DG, Nan B, Rohrer S, *et al*. Differentiation between brain tumor recurrence and radiation injury using MR spectroscopy. *AJR Am J Roentgenol* 2005;185(6):1471–1476.

[22] Chuang M-T, Liu Y-S, Tsai Y-S, Chen Y-C, Wang C-K. Differentiating radiation-induced necrosis from recurrent brain tumor using MR perfusion and spectroscopy: a meta-analysis. *PLoS One* 2016;11(1):e0141438.

[23] Zach L, Guez D, Last D, Daniels D, Grober Y, Nissim O, *et al*. Delayed contrast extravasation MRI: a new paradigm in neuro-oncology. *Neuro-oncology* 2015;17(3):457–465.

[24] Kano H, Kondziolka D, Lobato-polo J, Zorro O, Flickinger JC, Lunsford LD. T1/T2 matching to differentiate tumor growth from radiation effects after stereotactic radiosurgery. *Neurosurgery* 2010;66(3):486–491.

[25] Dequesada IM, Quisling RG, Yachnis A, Friedman WA. Can standard magnetic resonance imaging reliably distinguish recurrent tumor from radiation necrosis after radiosurgery for brain metastases? A radiographic-pathological study. *Neurosurgery* 2008;63(5):898–903.

[26] Stockham AL, Tievsky AL, Koyfman SA, Reddy CA, Suh JH, Vogelbaum MA, *et al*. Conventional MRI does not reliably distinguish radiation necrosis from tumor recurrence after stereotactic radiosurgery. *J Neurooncol* 2012;109(1):149–158.

[27] Essig M, Waschkies M, Wenz F, Debus J, Hentrich HR, Knopp MV. Assessment of brain metastases with dynamic susceptibility-weighted contrast-enhanced MR imaging: initial results. *Radiology* 2003;228(1):193–199.

[28] Kimura T, Sako K, Tohyama Y, Aizawa S, Yoshida H, Aburano T, *et al*. Diagnosis and treatment of progressive space-occupying radiation necrosis following stereotactic radiosurgery for brain metastasis: value of proton magnetic resonance spectroscopy. *Acta Neurochir* 2003;145(7):557–564.

[29] Seeger A, Braun C, Skardelly M, Paulsen F, Schittenhelm J, Ernemann U, *et al*. Comparison of three different MR perfusion techniques and MR spectroscopy for multiparametric assessment in distinguishing recurrent high-grade gliomas from stable disease. *Acad Radiol* 2013;20(12):1557–1565.

[30] Fink JR, Carr RB, Matsusue E, Iyer RS, Rockhill JK, Haynor DR, *et al*. Comparison of 3 Tesla proton MR spectroscopy, MR perfusion and MR diffusion for distinguishing glioma recurrence from posttreatment effects. *J Magn Reson Imaging* 2012; 35(1):56–63.

[31] Matsusue E, Fink JR, Rockhill JK, Ogawa T, Maravilla KR. Distinction between glioma progression and post-radiation change by combined physiologic MR imaging. *Neuroradiology* 2010;52(4):297–306.

[32] Zeng QS, Li CF, Liu H, Zhen JH, Feng DC. Distinction between recurrent glioma and radiation injury using magnetic resonance spectroscopy in combination with diffusion-weighted imaging. *Int J Radiat Oncol Biol Phys* 2007;68(1):151–158.

[33] Kickingereder P, Dorn F, Blau T, Schmidt M, Kocher M, Galldiks N, *et al*. Differentiation of local tumor recurrence from radiation-induced changes after stereotactic radiosurgery for treatment of brain metastasis: case report and review of the literature. *Radiat Oncol* 2013;8:52.

[34] Prat R, Galeano I, Lucas A, Martinez JC, Martin M, Amador R, *et al*. Relative value of magnetic resonance spectroscopy, magnetic resonance perfusion, and 2-(18F) fluoro-2-deoxy-D-glucose positron emission tomography for detection of recurrence or grade increase in gliomas. *J Clin Neurosci* 2010; 17(1):50–53.